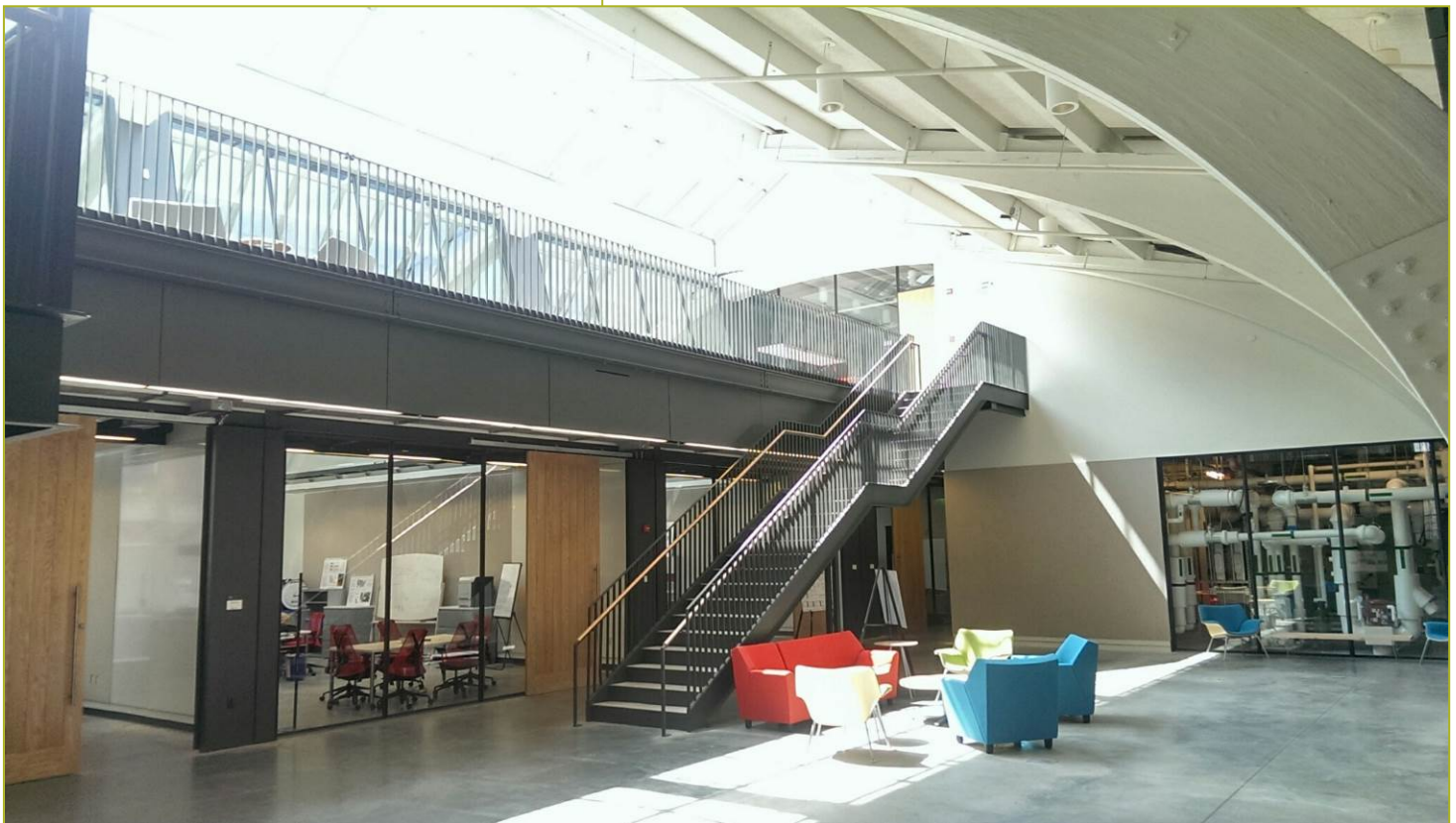**Title: Model Predictive Control and Fault Detection and Diagnostics of a Building Heating, Ventilation, and Air Conditioning System**

**Report Date: April 2014**

**Report Author(s):  Sorin Bengea, Pengfei Li, Soumik Sarkar, Sergey Vichik, Veronica Adetola, Keunmo Kang, Teems Lovett, Francesco Leonardi, Anthony Kelman**

## Report Abstract

This paper presents Model Predictive Control (MPC) and Fault Detection and Diagnostics (FDD) technologies, their on-line implementation, and results from several demonstrations conducted for a large-size HVAC system. The two technologies are executed at the supervisory level in a hierarchical control architecture as extensions of a baseline Building Management System (BMS). The MPC algorithm generates optimal set points for the HVAC actuator loops which minimize energy consumption while meeting equipment operational constraints and occupant comfort constraints.

## Contact Information for Lead Researcher

**Name:** Sorin Bengea
**Institution:** United Technologies Research Center

## Acknowledgement

## Disclaimer

# Model Predictive Control and Fault Detection and Diagnostics of a Building Heating, Ventilation, and Air Conditioning System

Sorin BENGEA[1]*, Pengfei LI[1], Soumik SARKAR[1], Sergey VICHIK[2], Veronica ADETOLA[1], Keunmo KANG[1], Teems LOVETT[1], Francesco LEONARDI[1], Anthony KELMAN[2]

[1]United Technologies Research Center, United Technologies Corporation, East Hartford, CT, USA
[2]Department of Mechanical Engineering, University of California, Berkeley, CA, USA

## ABSTRACT

The paper presents Model Predictive Control (MPC) and Fault Detection and Diagnostics (FDD) technologies, their on-line implementation, and results from several demonstrations conducted for a large-size HVAC system. The two technologies are executed at the supervisory level in a hierarchical control architecture as extensions of a baseline Building Management System (BMS). The MPC algorithm generates optimal set points for the HVAC actuator loops which minimize energy consumption while meeting equipment operational constraints and occupant comfort constraints. The MPC algorithm is implemented using a new tool, the Berkeley Library for Optimization Modeling (BLOM), which generates automatically an efficient optimization formulation directly from a simulation model. The FDD algorithm detects and classifies in real-time potential faults of the HVAC actuators based on data from multiple sensors. The performance and limitations of FDD and MPC algorithms are illustrated and discussed based on measurement data recorded from multiple tests.

## 1. INTRODUCTION

The large potential economic impact of advanced technologies underlying modern Building Management Systems (BMS) have led to increased efforts focused on developing, designing, and implementing model-based control and diagnostics technologies for building HVAC systems with the objective to estimate their cost effectiveness. The potential economic impact is apparent both from the high energy-consumption levels of building HVAC systems, estimated currently at 27% (EPA, 2008), and from limitations of existing control technologies for HVAC systems. To overcome current non-optimal performance and limited coordination capabilities, model-based paradigms have been employed to integrate in a direct and systematic way sensor data from multiple subsystems with the objective to generate optimal set-points that lead to and increased overall efficiency. Implementation of model-based algorithms—requiring more communication and computational resources than traditional control systems—has been facilitated by the availability of modern BMSs platforms and open communication infrastructures.

This paper describes a model-based optimal set-point control algorithm, MPC, and a data-driven equipment fault diagnostics implemented at supervisory level, as an extension of a baseline Building Management System (BMS). The focus is on their development, implementation, and performance estimation based on the results of tests conducted in two commercial buildings. Integration of the two technologies into the same model-based framework addresses two major challenges in building control systems: cost of deployment (relative to energy savings), and optimization of the HVAC system efficiency throughout its life. Although previous efforts (Adetola *et al.*, 2013; Bengea *et al.*, 2014) have demonstrated energy savings separately for diagnostics and optimal control algorithms at various building scales, the model-based technologies have not always led to cost-effective solutions due to the cost of commissioning of instrumentation and algorithms. The effort described herein minimizes these costs in two ways. First, by deploying the MPC and FDD algorithms on the same platform, within the same framework, using the same sensor suites for large-size HVAC units. Second, by employing an automated tool for formulating optimization problems associated with MPC algorithms. In addition, the integrated framework proposed herein has the potential to maximize the building system efficiency throughout its lifetime by enabling implementation of fault-tolerant technologies that integrate the two algorithms.

Fault detection and diagnostics technologies can potentially reduce significant energy inefficiency resulting from faults and degradation of building equipment and materials; errors in operating schedules and critical design/planning flaws. A comprehensive literature review can be found in (Katipamula 2005a, and 2005b) where the FDD methods are broadly categorized into two classes, namely model-based and data-driven. Model-based

techniques primarily involve either physics-based models, such as APAR rules in (Schein, 2006), sophisticated Modelica models in (Wetter 2009), EnergyPlus simulation models in (Pedrini *et al.*, 2002)) or empirical models, such as extended Kalman Filter in (Yoshida, 1996). Although model-based techniques perform reasonably well, often calibration and validation of such models may become expensive. Data-driven techniques have the advantage that require a reduced calibration and validation effort and range from simple statistical analysis (Seem 2007), principal component analysis (Xiao and Wang, 2009) to complex machine learning models, such as artificial neural network (Peitsman and Bakker, 1996). The algorithm implemented for this effort uses a probabilistic graphical-model based technique to model the historical performance of various HVAC subsystems in a data-driven manner. Specific faults of HVAC actuators, such as dampers and valves are flagged and diagnosed in real-time upon detections of any deviations from the modeled nominal behavior. Based on experimental data, it was estimated that the FDD algorithm correctly diagnosed the HVAC subsystem faults in 84% of the cases, missed the detection of 6% of the events, and generated false alarms in 10% of the cases when faults were seeded.

Model Predictive Control technologies are applied optimal control algorithms that use dynamical and steady-state models and predictions of plant disturbances to minimize a selected performance cost while satisfying operation and equipment constraints (Morari and Lee 1999; Mayne *et al.* 2000; Borrelli 2003). In this effort, an MPC algorithm was implemented at supervisory level to periodically solve an optimization problem and generate optimal sequences of set points for AHUs and VAVs. A similar hierarchical architecture has been proposed in (Kelly 1988). Simulation and experimental results have been reported previously for smaller scale HVAC systems (Henze *et al.* 2004, 2005, Clarke *et al.* 2002, Li *et al.* 2012), and for radiant HVAC systems (Siroky *et al.* 2011). A similar implementation of an MPC technology, as the one described here, was reported in (Bengea *et al.* 2014) for a medium-scale Multi-Zone Unit for a commercial building. The efforts presented in this manuscript build on this previous implementation by employing the Berkeley Library for Optimization Modeling (BLOM) (Kelman, Vichik, and Borrelli, 2013) to automatically formulate the MPC algorithm and implementing it for a large-scale building. This new tool significantly reduces the development effort of translating nonlinear simulation-oriented models into efficient constrained optimization problem formulations for MPC. The performance results estimated based on sensor measurements and meter data show that MPC algorithm reduced energy consumption by more than 20% while improving thermal comfort.

The paper is organized as follows. Section 2 describes the HVAC system configuration and the models used for MPC design. The FDD algorithm design and calibration are presented in the Section 3. Section 4 presents the MPC algorithm and the tool chain used to automate the optimization problem formulation. Experimental results and performance estimates based on test data are described in Section 5.

## 2. BUILDING HVAC AND CONTROL-ORIENTED MODELS

This section describes the building HVAC system used for testing the control and diagnostics algorithm, its configuration, and the served zones. It also details some of the models used by the applied optimal control algorithm.

### 2.1 Description of Building HVAC System
This section describes the main HVAC subsystems, their local control loops, and instrumentation. The HVAC system has a centralized architecture in which a steam-to-hot-water heat exchanger plant serves multiple AHUs in two identical large-size buildings located at the Navy Recruit Training Center, Great Lakes, IL. The HVAC systems consist of three Air Handling Units (AHU) serving 57 Variable Air Volume (VAV) units. Each of these AHUs serves 18 VAV units located in 9 compartments, each with a capacity of several tens of occupants, which are occupied during night-time. The temperature set point is based on a circadian variation, with higher set points (during cooling season) during night-time. This schedule is programmed in the BAS and is identical for all zones; there are not thermostats in the zones.

The focus of this effort in on AHUs and their VAVs which are instrumented as detailed in Table 1. The local control algorithms for each of the subsystems of Table 1 are based on PI and rules as described below:
- The VAV dampers $d_{VAV_i}$ and re-heat coil valves $v_{VAV_i}$ are controlled based on two coordinated Proportional-Integral algorithms and rules that are driven by the zone set point tracking error. The local controllers seek to

maintain the zone temperature within comfort bands $[T_{LB,S_i}, T_{UB,S_i}]$ that change at pre-scheduled intervals, and repeat every 24 hours. The discharge air temperature to each zone is controlled in open-loop (due to a lack of discharge air temperature sensors for most of the units). The volumetric air flow rate $\dot{V}_{VAV_i}$ is controlled by modulating the VAV damper $d_{VAV_i}$ to meet the scheduled set point.

- The AHU fan speed is controlled in order to maintain pressure set point scheduled in BAS. The by-pass face damper and the heating coil valve are controlled based on a loop that tracks a discharge air temperature set point. The OA damper is controlled to maintain a minimum MAT set point (during the heating season), which is coordinated with the freeze-protection control rule.
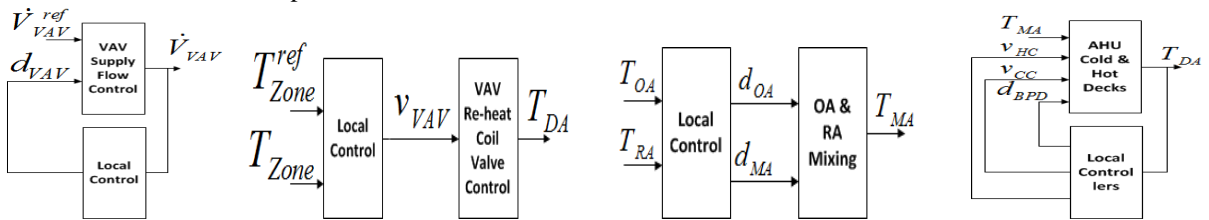


Figure 1. Signal flows of the VAV local control loops corresponding to supply air flow rate and zone temperature; Signal flows of the AHU local control loops corresponding to mixed air and discharge air temperatures

Table 1. Instrumentation of the HVAC systems

|  | AHU Instrumentation | VAV Instrumentation | Spaces |
|---|---|---|---|
| Common sensors (baseline installation) | • Discharge air, mixed air, and return air temperature sensors; damper and valve position sensors <br> • Fan VFD speed and power meter | • Volumetric air flow rate metering station <br> • Re-heat coil valve position sensor | • Zone temperature, $CO_2$ sensors |
| Special sensors instrumented for this effort | • One AHU was instrumented with BTU meters for both heating and cooling coils, and volumetric air flow rate metering station <br> • The same AHU was instrumented with more accurate averaging mixed and discharge temperature sensors <br> • Forecast of outdoor air temperature (downloaded on-line from NOAA) | • Three VAVs have been instrumented with BTU meters, inlet air temperature sensors, re-heat coil valve position sensors, and damper position sensors <br> • 18 VAVs have been instrumented with discharge air temperature sensors | • Zone relative humidity sensors |
| Common actuators | • Dampers: face by-pass damper, which controls the mixed air flow portion through the heating deck; outdoor air and return air dampers <br> • Heating and cooling coil valves | • Dampers <br> • Re-heat coil valves, | |

## 2.2 Control-Oriented Models

This section describes the models used for the MPC algorithm design. In view of the time-scale separation of the zone temperature dynamics (with a time response in the order of tens of minutes) and HVAC subsystems (with a time response at most a few minutes), the only dynamical model considered in this approach corresponds to the zone temperature dynamics. The following models are developed at steady-state: outdoor air fraction model; mixed air temperature model; AHU heating coil model; AHU total air flow rate model; AHU supply fan model; VAV re-heat coil model. All expressions considered in this model are polynomial in order to facilitate derivations of first and second order derivatives required for the optimization solver, as explained in Section 4.2.

After testing several ARMAX models (Auto-Regressive Moving-Average with External Disturbance), the following nonlinear ARX model was selecting for representing the dynamics of the zone temperatures:

$$T_{S_i}(k+1) = \alpha_1 T_{S_i}(k) + \alpha_2 T_{S_i}(k-1) + \alpha_3 T_{S_i}(k-2)$$
$$+ \beta_1 T_{OA}(k) + \beta_2 T_{OA}(k-1) + \gamma \ \dot{m}_{sa,S_i}(k)\left[T_{sa,S_i}(k) - T_{S_i}(k)\right] + d_{S_i} \tag{1}$$

where we used the notation as defined in the Section Nomenclature, the sampling time is 5 minutes, and parameters $\alpha_{S_i,1}, \alpha_{S_i,2}, \alpha_{S_i,3}, \beta_{S_i,1}, \beta_{S_i,2}, d_{S_i}$ are identified using several measurement tests. A subset of the measurement sets was generated from experiments designed with selected input profiles; another subset was selected from historical data. The controlled test inputs are AHU heat coil valve position $v_{AHU,HC}$, the VAV re-heat coil valve positions $v_{VAV_i,HC}$, and the VAV supply air flow rates $\dot{m}_{sa,S_i}$; a set of data is illustrated in Figure 2 (left). Although these tests were applied to all three AHUs and their corresponding VAVs, a model was used to generate estimates of VAV discharge air temperatures $T_{sa,S_i}(k)$ for the VAVs which were not instrumented with these additional sensors. The ability of the models to predict zone temperature was subsequently evaluated using new sets of data. Such a set of data is illustrated for one zone in Figure 2 (right).
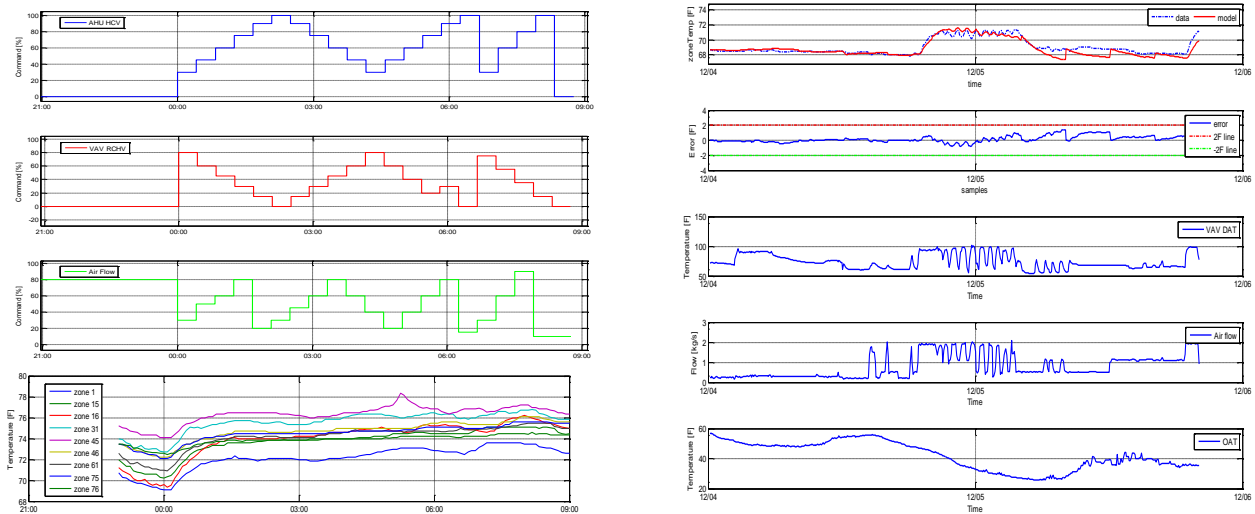


Figure 2. (Left) Normalized time series data of the inputs $v_{AHU,HC}$, $v_{VAV_i,HC}$, and $\dot{m}_{sa,S_i}$ for a system identification test for AHU$_1$, and corresponding zone temperatures measurements; (Right) Model validation results using new data sets based on which it was concluded that the zone temperature modeling error is smaller than $2^0$F

Table 2. HVAC steady-state models and assumptions

| HVAC Subsystems | Assumptions | Equations |
|---|---|---|
| Outdoor air fraction and mixed-air temperature | • Steady-state models as functions of outdoor air damper, specifically for heating season | $f_{OA} = c_{2,OA} \cdot d_{OA}^2 + c_{1,OA} \cdot d_{OA} + c_{0,OA}$ <br> $T_{MA} = f_{OA} \cdot T_{OA} + (1 - f_{OA}) \cdot T_{RA}$ |
| Thermal power of AHU heating coil | • Steady-state models as functions of volumetric air flow rate, inlet and discharge air temperatures | $P_{HC} = \dot{m}_{SA} \cdot c_{pa} \cdot (T_{DA,AHU} - T_{MA} - \Delta T_{SF})$ |
| AHU supply air flow rate | • Constant air flow leakages in the supply ducts to zone VAVs | $\dot{m}_{SA,AHU} = c_{1,SA} \cdot \sum_i \dot{m}_{SA,VAV_i} + c_{0,SA}$ |
| Electrical power of supply fan | • Function of supplied air flow | $P_{SF} = c_{3,SF} \cdot \dot{m}_{SA,AHU}^3 + c_{2,SF} \cdot \dot{m}_{SA,AHU}^2$ <br> $+ c_{1,SF} \cdot \dot{m}_{SA,AHU} + c_{0,SF}$ |
| Thermal power of VAV re-heat coils | • Steady-state models as functions of volumetric air flow rate, inlet and discharge air temperatures | $T_{SA,VAV} = T_{SA,AHU} + c_{3,VAV} \cdot \dfrac{T_{W,HC,in}}{\dot{m}_{SA,VAV}^{c_{2,VAV}}} \cdot v_{HC}^{c_{1,VAV}}$ |

All HVAC subsystem control-oriented models are determined at steady-state due to their faster time response (one order of magnitude) relative to the zone temperature dynamics. The HVAC subsystems, their models and main assumptions are included in Table 2 (using the notation described in the Nomenclature section).

All the steady-state models of Table 2 have been calibrated and validated with multiple sets of data. The histograms of the validation errors, between model predictions and measurements, are illustrated in Figure 3. Constraints related to the size of this paper preclude inclusion of additional time series data and more detailed discussions of the assumptions and restrictions of these models.
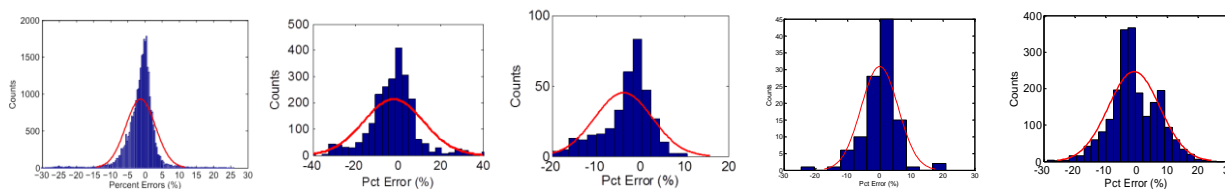


Figure 3. Histograms of the validation errors for all models of Table 2 (in the same order as in the table: mixed-air temperature; AHU heating coil thermal power; AHU supply air flow rate; AHU supply fan power; VAV re-heat coil thermal power)

# 3. FAULT DETECTION AND DIAGNOSTICS ALGORITHMS

This section describes the implemented FDD system which uses a data-driven methodology integrated with domain knowledge to detect and diagnose faults. The FDD tool-chain includes a data-driven, off-line step of learning the nominal behaviors and an on-line step of detecting off-nominal behaviors. Data-driven methodologies have several advantages, such as low-cost commissioning, scalability, adaptability to system variation/evolution, and limited requirement of domain knowledge. The selected data-driven method consists of a graphical-network-based approach which allows encoding the background domain knowledge and physics-based understanding of the system, while allowing discovery of new relationships within data streams using structure learning algorithms.

The FDD tool-chain used in this project primarily has the following steps:
- Data acquisition. Data-driven methods require sufficient data in order to reliably model a complex system. Data sufficiency involves two major aspects: spanning the operating space, and statistically significant amount of data. Both historical data and functional tests have been used in order to generate enough data to model discrete graphical models for different building subsystems.
- Data pre-processing. The two major steps are: data quality verification, and data abstraction for modeling. In the data quality verification step, sensor observations are checked for data ranges, rate of changes and communication reliability. In order to prepare data for discrete probabilistic graphical models, continuous sensor observations were discretized using various techniques including equal-width, equal frequency and Maximally Bijective Discretization (Sarkar *et al.* 2013).
- Model learning. The graphical structure of the FDD model is learned in an exclusively data-driven manner to discover relationships between variables inherent in the data. The structure is then validated against domain knowledge and physics based understanding of the system. Using a goodness-of-fit metric that is based on accuracy of prediction of selected critical variables, model parameters are adjusted to achieve a good fit. The graphical network model for FDD is used to analyze new validation data to generate an anomaly score quantifying the extent of departure from the nominal performance of variable, given the measurement of other related variables. Based on the anomaly scores and a suitably chosen threshold, faults can be detected in any variable of the FDD model. The flagged events were then verified against ground truth.
- On-line detection. Probabilistic graphical models are built for each relevant building sub-system.

The developed FDD algorithms and their graphical representations are discussed and illustrated in Table 3 and Figure 4, respectively. The graphical network models were calibrated and validated using multiple sets of data generated by overriding the BAS commands. Figure 5 contains the results of a validation test for the FDD algorithm associated with the $d_{OA}$ damper. In this case a fault was seeded by overriding the damper command to 85% open,

while the BAS command was only 40%. Using the sensor information from several temperature sensors, the FDD algorithm detected correctly the seeded faults.

Table 3. FDD approach details corresponding to AHU subsystems

| Subsystem | Faults | FDD graphical model nodes |
|---|---|---|
| VAV terminal unit | • Damper $d_{VAV_i}$ : stuck; air leakages; sticky<br><br>• Valve $v_{VAV_i,HC}$ : stuck; leakages; sticky | Damper position, supply air flow rate, heating coil valve position, and air flow thermal power |
| AHU | • Damper $d_{OA}$ : stuck; air leakages; sticky | Damper position, estimated outdoor-air flow fraction (based on temperature measurements) |
| | • Valve $v_{AHU,HC}$ : stuck; water leakages; sticky | Heating coil valve position, air flow thermal power, air flow rate, face by-pass damper position, difference between inlet and outlet water temperatures |
| | • Fan: capacity and efficiency changes | Fan speed, electrical power, supply static pressure, air flow rate |
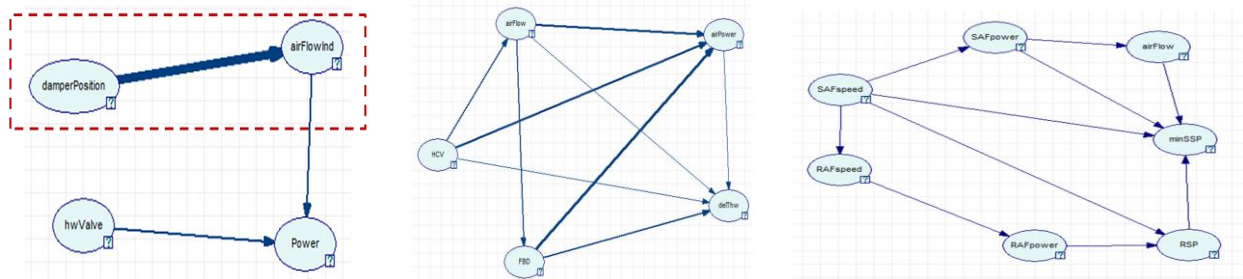


Figure 4. Graphical FDD models for the following actuators: outdoor air damper (left);
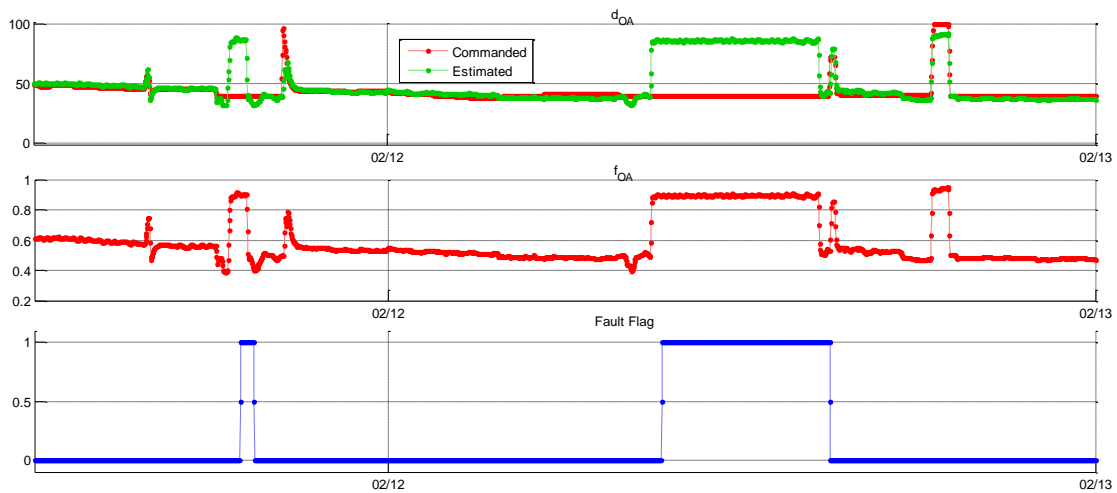AHU heating coil (center); AHU fans (right)



Figure 5. Illustration of validation test data for the FDD algorithm associated with outdoor air damper
Outdoor air damper: BAS command, which was overridden; estimated position (top); outdoor air fraction (middle);
fault flag (bottom)

A small delay in generating the fault flag is observed and this is implemented in the algorithm to ensure that the fault persists for some time before it is flagged, and therefore reduce potential false alarms. More experimental data sets are presented and discussed in Section 5.

# 4. MODEL PREDICTIVE CONTROL AUTOMATED FORMULATION AND IMPLEMENTATION

This section describes the MPC problem, the hierarchical control architecture in which it is implemented, and the automated tool chain employed for its formulation.

## 4.1 Model Predictive Control Formulation

An MPC algorithm is implemented to generate real-time optimal set points for the building HVAC subsystems by searching for the most energy efficient control input sequences subject to system constraints (thermal comfort, component performance) and disturbances (weather, internal loads), similarly to the implementation in (Bengea *et al.* 2014). The MPC algorithm is implemented at the supervisory level in a hierarchical architecture whose signal flow is illustrated in Figure 6.
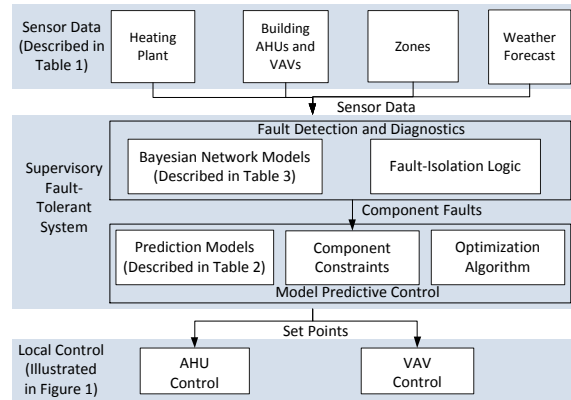


Figure 6. Hierarchical architecture of the fault-tolerant system

The MPC formulation integrates in the same framework the control-oriented building-system performance and zone-temperature models described in Table 2, and operational and thermal comfort constraints. The algorithm is formulated as a deterministic optimization problem as described below, where we use the same notation as in Section Nomenclature and all the models are described in Section 2.2. The problem is formulated separately for each AHU and served VAVs and spaces.

$$\text{Objective cost:} \quad Min \sum_{t_0}^{t_f} \left\{ \sum_{VAV_i} \left[ P_{AHU,HC} + P_{AHU,SF} + P_{VAV_i,HC} + Penalty(T_{S_i}, T_{S_i,UB}, T_{S_i,LB}) \right] \right\} \quad (2)$$

Optimization variables (21 control inputs):
VAV air flow rates $\dot{m}_{VAV_i,SA}^{ref}$ and re-heat coil valve positions $v_{VAV_i,HC}$, AHU discharge air temperature $T_{AHU,DAT}^{ref}$, and damper positions $d_{OA}$ and $d_{MA}$

Subject to: Equality constraints for AHU, VAVs, and zone temperatures from Table 2

$$T_{AHU,DAT}^{ref} \le T_{AHU,DAT}^{max}(T_{MA}, \dot{m}_{SA,AHU}) \quad (3)$$

AHU inequality constraints
$$\dot{m}_{AHU,SA} \le \dot{m}_{AHU,SA}^{max} \quad (4)$$

$$d_{OA,min} \le d_{OA} \le 1, \ 0 \le d_{MA} \le 1, \ 0 \le v_{AHU,HC} \le 1 \quad (5)$$

VAV inequality constraints
$$\dot{m}_{VAV_i,SA} \le \dot{m}_{VAV_i,SA}^{max} \quad (6)$$

$$0 \le v_{VAV_i,HC} \le 1 \quad (7)$$

The lower and upper bounds $d_{OA,min}$ is preset as an operation constraint. The comfort constraints are formulated as soft constraints via function $Penalty(T_{S_i}, T_{S_i,UB}, T_{S_i,LB})$ in (2), which penalizes the excursions of the zone temperature outside of the comfort band $[T_{S_i,LB}, T_{S_i,UB}]$ which is scheduled for each zone and is time-dependent.

The soft-constraint formulation does not causing any infeasibility issues when some zone temperatures may leave the comfort band (e.g. due to different actual loads than forecasted).

The above optimization problem is solved at 15 minute time intervals and consists of: updating the sensor measurements and weather forecast; estimating temperature states; diagnosing component faults; generating optimized set-points for the entire four-hour prediction horizon; communicating the new set point values (only for the next sampling time) to BMS. This repeated calculation of set points ensures solution robustness and optimality by using the most recent measurements and outdoor temperature forecasts.

The optimization problem formulation workflow—the process by which the above mathematical problem is converted into an optimization algorithm— is illustrated in Figure 7.

## 4.2 Automated Optimization Problem Formulation

The MPC algorithm formulated in Section 4.1 was converted into an optimization problem by using The Berkeley Library for Optimization Modeling (BLOM) (Kelman *et al.* 2013). BLOM bridges the gap between simulation oriented tools (Simulink, Modelica, etc.) and optimization oriented tools (Kallrath 2004, Soares *et al.* 2003). BLOM is based on a new formulation for representing linear and nonlinear mathematical functions that aims to address some of the limitations of simulation-oriented tools. This formulation allows for direct computation of closed form gradients, Jacobians and Hessians. The initial model formulation interface is based on Simulink, and BLOM provides a set of Matlab functions which transform a Simulink model into an optimization problem using our representation format. This problem representation is then used in a compiled interface to an optimization solver such as IPOPT (Wächter *et al.* 2006). BLOM consists of three main parts. First, there is the Simulink front end, where a dynamic model is represented using built-in Simulink blocks and the BLOM library blocks. Second, a set of Matlab functions is used to convert a Simulink model into the internal mathematical representation described in (Kelman *et al.* 2013). Lastly, this problem representation is used by an interface to an optimization solver such as IPOPT. The BLOM front end for Simulink includes (in addition to the regular Simulink blocks) inequality, cost function, and designation of variables as free optimization variables or set by a user.

As shown in Figure 7, first, a model is created in Simulink and validated using forward simulation. Second, the model is converted to an optimization problem and exported to a solver (IPOPT). Third, a problem data is supplied and a solution is obtained. The third step is repeated, with a new state measurement every time step. For efficient online solution of a large nonlinear MPC optimization problem in real time, it is critical that the sparsity structure of both the spatial connectivity in the model and the temporal causality over the MPC prediction horizon are captured and represented in the optimization formulation. BLOM is designed using an efficient sparse nonlinear problem representation in order to capture this information from the system model in a way that the optimization solver can fully utilize.
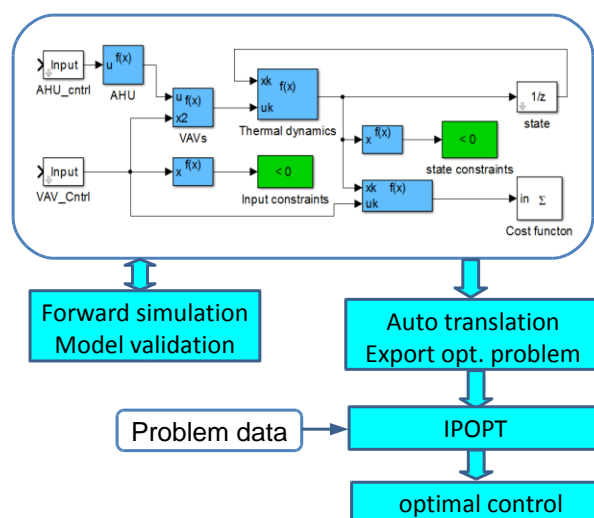


Figure 7. The main steps for converting the MPC algorithm into an optimization problem formulation using BLOM

Table 4 presents typical performance of the BLOM library with IPOPT solver for the MPC problem formulated in Section 4.1. We present the execution time of problem solution for various problem sizes. The table shows that even

for very large problems with more than 10000 variables and constraints, the library achieves good performance and IPOPT converges quickly to a Karush-Kuhn-Tucker point of the constrained finite-time optimal control problem.

Table 4. BLOM execution results

| Prediction horizon length (steps) | 20 | 30 | 50 |
|---|---|---|---|
| Number of variables in solver | 11180 | 16770 | 27950 |
| Number of constraints | 8777 | 13252 | 22202 |
| Non-zeros in Jacobian and Hessian | 31682 | 48227 | 81317 |
| Number of solver iterations | 91 | 142 | 128 |
| Total solution time [sec] | 6.6 | 20.3 | 46.8 |
| Time spent in BLOM callbacks | 34% | 30% | 29% |

## 5. EXPERIMENTAL RESULTS AND PERFORMANCE ESTIMATION

This section presents the performance estimates generated based on multiple test conducted from Nov. 2012 to March 2013 for three AHUs. The performance results are described separately for the FDD and MPC algorithms. The section starts with a description of the method employed to estimate the overall system performance, then describes aggregated performance results, continue with plots of experimental data for both FDD and MPC algorithms and concludes with a discussion of the limitations of this performance analysis.

### 5.1 Performance Estimation for the MPC and FDD Algorithms
The main performance metrics addressed in this effort are: overall energy consumption, peak power, comfort, and percentage of faults identified correctly. The overall energy (power) consumption was calculated using both electrical energy (power) consumption (for fans) and thermal energy (power) consumption for heating heat exchangers. The overall energy (power) consumption was estimated by converting the thermal component to an electrical component using the estimated Coefficient of Performance (COP) of the heating plant. The comfort criteria was initially intended to be addressed as a hard constraint (as a band around zone thermostat set points), but it was observed that the baseline control algorithms did not meet this constraint for several time intervals every day. Therefore a more realistic criteria was used that estimates comfort violations (during the heating season) as

$$\int_{t_0}^{t_f} \max(0, T_{S_i,LB}(t) - T_{S_i}(t))dt \tag{8}$$

which represents the accumulated time interval over which the comfort constraint is not met (during the heating season) weighted by the level of constraint violation.

We present first the overall results generated based on the sensor and meter data recorded from the demonstrations conducted during the heating season 2012-13. The overall results are illustrated in Figure 8 for each AHU, relative to the baseline BAS schedule performance; the performance targets are illustrated as horizontal red lines.

The overall FDD algorithm performance was estimated using sensor and meter data recorded during multiple test windows. Based on this data, it was estimated that the FDD algorithm correctly diagnosed the HVAC subsystem faults in 84% of the cases (level illustrated in Figure 8), missed the detection of 6% of the events, and generated false alarms in 10% of the total events which consist of equal number of seeded and non-seeded (real) faults. The seeded faults were implemented by overriding the commands communicated by the controllers (with the BACNet message priority set at a value that enables the override), without communicating these overrides to the FDD algorithm. An example of a correctly diagnosed damper fault is illustrated in Figure 9 were the trained VAV FDD algorithms correctly diagnosed the damper-stuck faults. Upon this fault diagnostics, this particular fault was confirmed by investigated the actual VAVs.
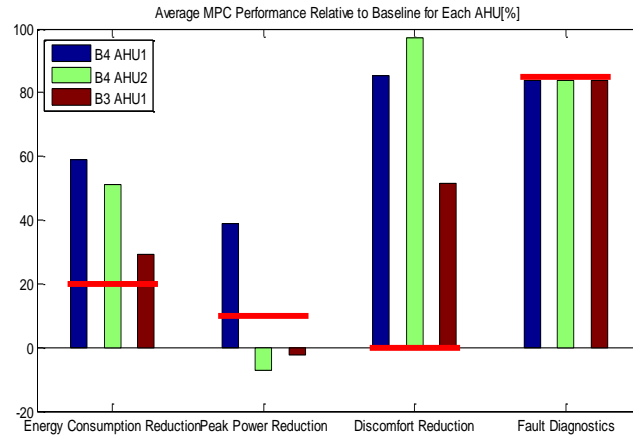
Figure 8. Illustration of the overall results generated during the demonstrations for MPC and FDD algorithms for each of the AHUs for the following objectives: energy consumption reduction, peak power reduction, thermal discomfort reduction, and fault diagnostics system robustness.
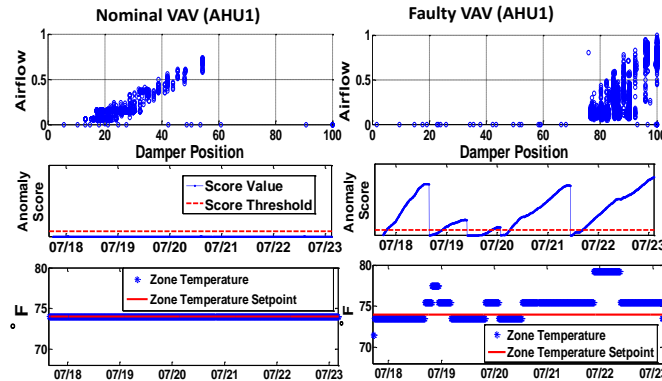


Figure 9. Comparisons between nominal (healthy) and faulty VAV units

The lack of sufficient instrumentation and the inaccuracy of sensors for building HVAC systems present significant challenges that result occasionally in miss-detection or false positive classifications. Particularly for high capacity HVAC units, with large air duct diameters, the inaccuracies of air temperature sensors at different location can result in false positive FDD outcomes. Several data sets are illustrated in Figure 10, where the following inconsistencies are observed: (i) when $d_{OA}$ closes, $T_{MA}$ increases and gets closer to $T_{RA}$ as expected, but there are also time intervals over which $T_{MA}$ exceeds $T_{RA}$ ; (ii) $T_{MA}$ exceeds $T_{HR}$ when $d_{OA}$ is fully open; (iii) $T_{MA}$ exceeds $T_{HR}$ and $T_{RA}$ , which have similar values, by about $5^0$F. In all these cases, the FDD algorithm can trigger false alarms on some time sub-intervals. The limited sensor set data cannot be used to distinguish between multiple cases: mis-calibrated sensors; leakages that depend nonlinearly on damper positions; non-mixed air flows with non-uniform temperatures. In view of these limitations, the outdoor air damper faults that are seeded correspond to large variations in $d_{OA}$ in the interval [30%, 70%] opening; where the lower bound is imposed by fresh air constraints, and the upper bound was selected to avoid case (ii) discussed above. With this limited range on the outdoor air damper seeded-faults, which minimize the rate of false alarms for this damper, the false alarms are mostly generated for cases when large changes in set point values occur.
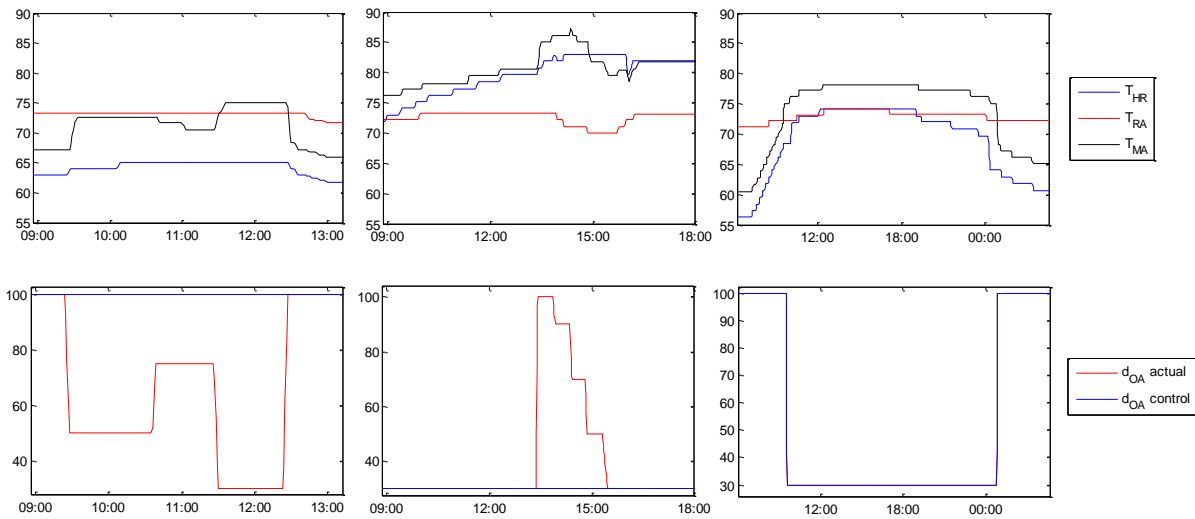
Figure 10. Illustration of the outdoor air damper positions and impacted temperatures for three scenarios described above the figure

For each AHU$_i$, $i = 1,2,3$, the results in Figure 8 are generated by averaging its performance over all demonstration days using the following formula for energy savings, peak power reduction, and thermal discomfort:

$$PerfMetric(AHU_i) = \frac{1}{N_{AHU_i,MPC}} \sum_{MPC_j} \left[ \frac{1}{N_{AHU_i,Baseline}} \sum_{Baseline_k} \left( 1 - \frac{PerfMetric(AHU_i, MPC_j)}{PerfMetric(AHU_i, Baseline_k)} \right) \right] \quad (9)$$

which calculates two averages: the first is across all MPC algorithm demonstration days, $MPC_j$, and the second is for all the baseline days $Baseline_k$ (during which the HVAC system is controlled by the baseline algorithm) that are selected to be compared against the performance results generated in $MPC_j$ demonstration day. This selection is discussed in the following.

In lack of sufficient large sets of test data, a criteria has to be used for selecting specific baseline days and MPC demonstration days for conducting performance analysis. The criteria selected for this analysis is based on ambient temperature; this selection was based on the assumption that, in lack of occupancy data, as is the case with many demonstration sites, the ambient conditions generate the largest disturbances that have to be rejected by HVAC system. Such a selection is illustrated in Figure 11 (left) where the ambient-temperature time series data for one MPC day and the corresponding baseline days are plotted.
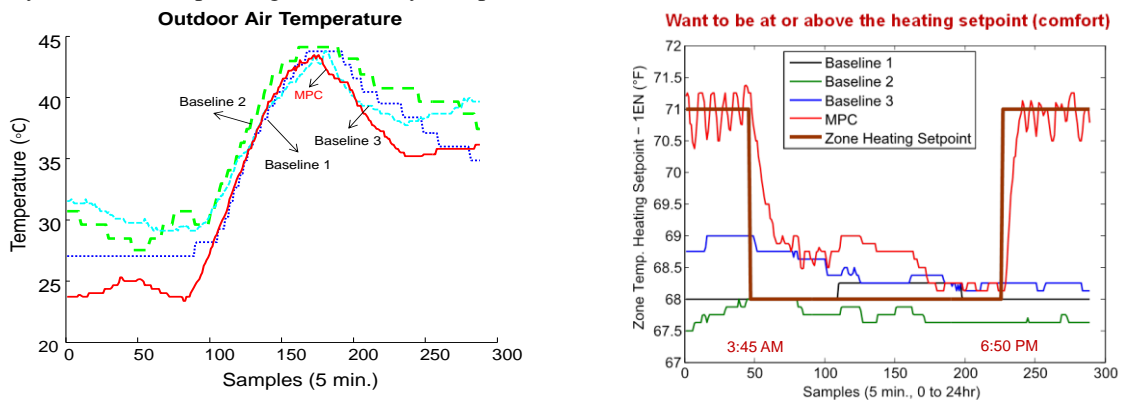
Figure 11. Illustration of ambient temperature during an MPC demonstration day (red) and selected baseline days with similar ambient temperature pattern (left). Temperature values corresponding the MPC and baseline controllers for the same days (right).

The same figure also illustrates (right plot) the zone temperatures generated with the corresponding algorithms during the same days as selected in the left plot. The performance of the MPC algorithm and the baseline algorithms during these days is further detailed in Figure 12 which illustrates that the baseline algorithms does not meet comfort when the set point values are changed (according to the circadian schedule implemented in BAS). In order to meet the thermal comfort constraint when the set point value is increased (during heating season) the MPC algorithm's peak power value exceeded the baseline algorithm's peak power values.
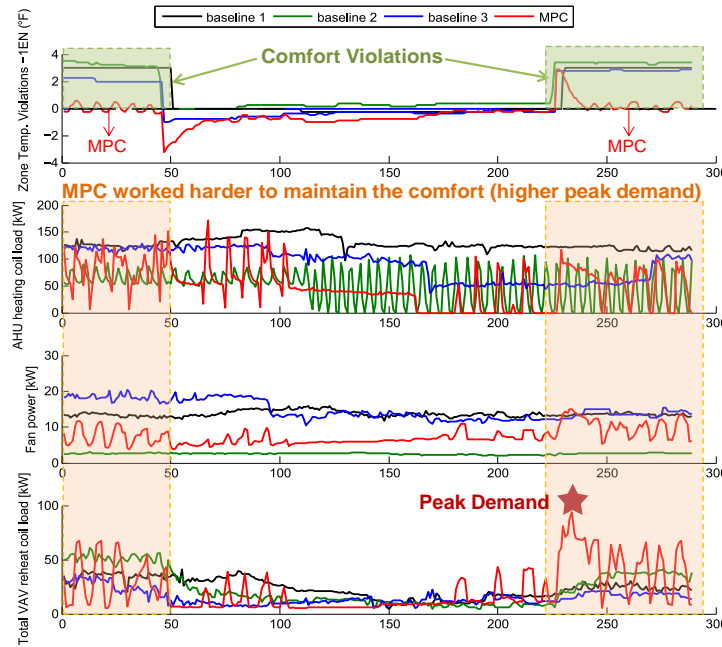


Figure 12. Illustration of temperature comfort violations, AHU heating coil power, fan power and total VAV thermal power during the same days as those illustrated in Figure 11.

The bar graphs in Figure 13 and 14 further illustrate a subset of the test data based on which the performance metrics in Figure 8 where calculated (using formula (9) and three baseline days with closest ambient temperature values for each MPC day). Energy consumption and peak power reduction levels are illustrated in Figure 13, where negative values in the peak power bar graph mean that MPC algorithm used higher power levels. The mean zone $CO_2$ levels and comfort violations are illustrated in Figure 14.
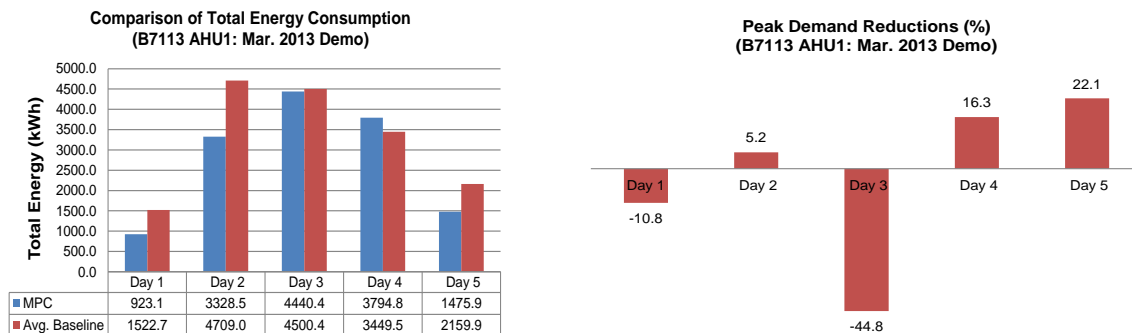


Figure 13. Total energy consumption and peak power reductions of MPC and baseline algorithms
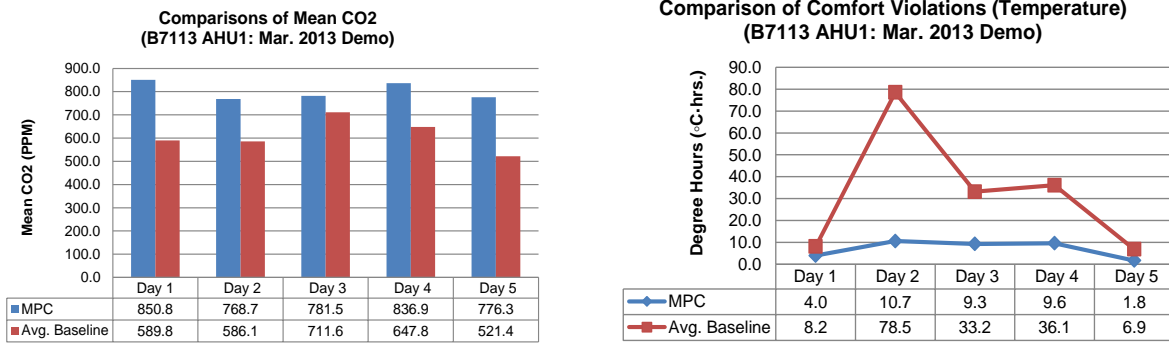
Figure 14. Mean zone $CO_2$ levels and temperature comfort violation levels for MPC and baseline algorithms

## 5.2 Limitations of the Performance Estimation Method

There are several limitations in the calculation of the performance estimates of the FDD and MPC algorithms and these are reviewed and discussed below for each algorithm. For FDD algorithm these limitations are consequences of the following factors:

- Only single faults are considered in this effort, and they are exclusively assigned to actuator faults; except for these faults, the HVAC units were considered otherwise healthy. As previously mentioned, it is not possible to distinguish between all possible faults that can occur with a limited sensor and meter data set.
- HVAC control systems have a large degree of fault-accommodation without explicitly estimating any faults. An example is discharge air temperature control loop at AHU level which controls the volume flow rate of the mixed airflow through the heating coil deck and the heating valve position. Even in the presence of faults associated with any of these two actuators, their local controllers can maintain a desired discharge air temperature set point. However, a large number of combinations between this flow rate and the heating valve positions can lead to the same temperature differences between the mixed air and discharged air. Without intermediate sensors for measuring the inlet temperature to the heat exchanger, an FDD algorithm has limited information for detecting any faults associated with these two actuators when using only data generated with the local controllers.
- The FDD performance reported in Figure 8 corresponds only to the units that were instrumented with additional sensors (as described in Table 1).

The estimation of the uncertainty magnitude in the reported performance levels of the MPC algorithm is limited by factors related to sensor instrumentation and test data size:

- Although the performance levels are estimated using measurement data from 26 days distributed unevenly during the entire heating season 2012-13, it is unclear whether the distribution of the internal loads and ambient conditions was representative for all heating seasons in the selected buildings. The level of sensor instrumentation needed to generate these estimates is beyond the level of instrumentation in standard commercial buildings, such as those used as for demonstrations for this effort. Therefore an extrapolation of the results in Figure 8 to other heating seasons, ambient conditions, or usage patterns cannot be made directly. We note, however, that large levels of energy savings were also demonstrated for a smaller AHU, similar ambient conditions, and different HVAC configuration and usage patterns (Bengea *et al.* 2014).
- The method used for MPC performance estimation is based on the assumption that the largest disturbance is ambient temperature, and therefore similarity in the outdoor air temperature patterns is the most important criteria when selecting multiple sets of days for performing energy consumption comparisons. When sufficiently large sets of data available, using multiple criteria would increase the accuracy of the performance estimates.
- Less than 30% of the models are validated. Due to limited sensor instrumentation for two of the AHUs ("B4 AHU2" and "B3 AHU1" in Figure 8), the AHU and VAV heat exchanger models could not be validated. Therefore the VAV re-heat coil energy consumption for these AHUs were estimated using the same models as those used for the AHU for which additional sensors were instrumented (as described in Table 1).
- The MPC algorithm does not use zone occupancy models and therefore does not control directly the $CO_2$ levels in the zones. The MPC algorithm met the minimum outdoor air damper constraint (designed for the baseline algorithm to meet the fresh air requirements). However, after the demonstrations it was observed that the MPC

algorithm consistently increased this level in all zones by about 35% on average (across all zones served by all three AHUs). The limitations in the sensor and meter data prevent detailed estimation of specific portions of the reported energy consumption levels in Figure 8 that are due to decreasing the outdoor air damper position (while still meeting the minimum damper-position constraint), meeting different occupancy loads, and increasing thermal comfort.

## 8. CONCLUSIONS

The paper presents the design, implementation, and performance results of two model-based algorithms based on tests conducted in two large-size commercial buildings during the heating season 2012-13. The MPC algorithm uses sensor data to generate periodic updates of AHU and VAV unit set point values that reduce energy consumption while maintaining all zones temperatures within a comfort band. The FDD algorithm uses sensor and meter data to isolate on-line faults associated with the AHU actuators. The individual performance benefits of the two algorithms are estimated based on test results compared against historical baseline data generated during test periods with similar ambient conditions. Although the energy performance depends on uncertainties which cannot be completed characterized with limited data, the results demonstrate the potential of the algorithms to reduce energy levels to levels that provide favorable cost benefits.

## NOMENCLATURE AND MATHEMATICAL NOTATIONS

| | |
|---|---|
| AHU | Air Handling Unit |
| BLOM | Berkeley Library for Optimization Modeling |
| BMS | Building Management System |
| CFM | Cubic Feet per Minute |
| $CO_2$ | Carbon Dioxide |
| COP | Coefficient of Performance |
| FDD | Fault Detection and Diagnosis |
| FTC | Fault-Tolerant Control |
| GPM | Gallon per Minute |
| HVAC | Heating, Ventilation and Air Conditioning |
| IPOPT | Interior Point OPTimizer |
| MPC | Model Predictive Control |
| NOAA | National Oceanic and Atmospheric Administration |
| VAV | Variable Air Volume |
| VFD | Variable Frequency Drive |
| $\dot{m}_{sa,S_i}$ and $T_{sa,S_i}$ | Mass flow rate and temperature of supplied air to space $S_i$ |
| $T_{OA}$, $T_{MA}$, $T_{RA}$ | Temperatures of Outdoor Air (OA), Mixed Air (MA), and Return Air (RA), respectively |
| $T_{S_i}$, $T_{S_i,UB}$, $T_{S_i,LB}$ | Air temperature in space $S_i$ and upper (set point during cooling season) and lower (set point during heating season) bounds of the temperature comfort band for space $S_i$ |
| $d_{OA}$, $d_{MA}$, $d_{RA}$, $d_{FBD}$ | Damper positions for Outdoor Air (OA), Mixed Air (MA), Return Air (RA), and by-pass air flow streams, respectively |
| $T_{sa,AHU}$, $T_{HD}$ $T_{CD}$ | Temperature of air supplied by AHU (downstream of hot and cold decks; upstream of VAV units); Temperature air discharged at the outlet of the hot and cold decks, respectively |
| $f_{OA}$ | Ratio between mass flow rate of outdoor air flow and mass flow rate of the mixed air flow |
| $v_{AHU,HC}$, $v_{VAV,HC}$ | Normalized position of the heating coil valve (the subscript makes it clear whether this belongs to the AHU heating coil of VAV re-heat coil |
| $P$ | Power (thermal or electrical) |

# REFERENCES

Adetola, V., Ahuja, S., Bailey, T., Dong, B., Khawaja, T., Luo, D., O'Neil, Z., Shashanka, M., 2013, "Scalable Deployment of Advanced Building Energy Management Systems", ESTCP-EW-1015 Project, Technical Report.

Atanu Talukdar & Amit Patra. Dynamic Model-Based Fault Tolerant Control of Variable Air Volume Air Conditioning System. HVAC&R Research Vol 16 (2), 2010. Pgs 233-254

Baotic, M., F. Borrelli, A. Bemporad, and M. Morari. "Efficient on-line computation of constrained optimal control". SIAM Journal on Control and Optimization, 5:2470–2489, September 2008

Bengea, S., Kelman, A., Borrelli, F., Taylor, R., and Narayanan, S., 2014, "Implementation of model predictive control for an HVAC system in mid-size commercial building", Journal of HVAC & R Research, Volume 20, Issue 1, pp. 121-135, 2014.

Borrelli, F., J. Pekar, M. Baotic and G. Stewart. "On The Computation Of Linear Model Predictive Control Laws". Automatica, 46(6):1035-1041, June 2010.

Borrelli, F., "Constrained Optimal Control of Linear and Hybrid Systems", Lecture Notes in Control and Information Sciences, vol. 290. Springer, 2003.

Bourassa, N., Automatic Diagnosis for Ailing Rooftop Air Conditioners, PIER Technical Brief, July 2005.

Brand, M.E., Pattern Discovery via Entropy Minimization. In Uncertainty 99: AISTATS 99, 1999.

Brand, M.E., Structure Learning in Conditional Probability Models via an Entropic Prior and Parameter Extinction in Neural Computation Journal, Vol. 11,No. 5, pp. 1155-1182, July 1999.

Chiang, L., E. Russell, R. Braatz, Fault Detection and Diagnosis in Industrial Systems, Springer Verlag, London, 2000.

Dudley, J.H., Black, D., Apte, M., Piette, M.A. and Berkeley, P. 2010. Comparison of Demand Response Performacnr with an EnergyPlus Model in a Low Energy Campus Building. 2010 ACEEE Summer Study on Energy Efficiency in Buildings. Pacific Grove, CA. August 15-20, 2010.

Environmental Protection Agency, 2008, Report on Environment, Final Report EPA/600/R-07/045F. United States Environmental Protection Agency.

Fernandez, N; Brambley, MR and S. Katipamula. Self-Correcting HVAC Controls: Algorithm for sensors and Henze, G., D. Kalz, C. Felsmann, and G. Knabe. 2004. "Impact of forecasting accuracy on predictive optimal control of active and passive building thermal storage inventory." HVAC&R Research, Vol. 10, No. 2, pp. 153–177.dampers in air handling units, US DOE report 2009 (Contract DE-AC05-76RL01830)

Henze, G.P., Kalz, D. E., Liu, S., and Felsmann, C., Experimental Analysis of Model-Based Predictive Optimal Control, HVAC&R Research, Vol. 11, No. 2, 2005, pp. 189-213.

Kallrath, J., Modeling Languages in Mathematical Optimization, ser. Applied Optimization. Kluwer Academic Publishers, 2004.

Kelly, G. 1988. "Control system simulation in North America". Energy and Buildings Vol. 10, pp. 193–202.

Kelman, A., Vichik, S., Borrelli, F., "BLOM: The Berkeley Library for Optimization Modeling and Nonlinear Predictive Control", Internal report, Department of Mechanical Engineering, University of California, Berkeley, 2013. Website: http://www.mpc.berkeley.edu/software/blom

Li, P., Baric, M., Narayanan, S., and Yuan, S. 2012, A Simulation-Based Study of Model Predictive Control in a Medium-Sized Commercial Building, *2nd International High Performance Buildings Conference at Purdue*, July 16-19, 2012, West Lafayette, IN.

Ljung, L., "System Identification: Theory for the User", Prentice Hall

Ma, Y., Borrelli, F., Hencey, B., Coffey, B., Bengea, S., Packard, A., Haves, P., "Model Predictive Control for the Operation of Building Cooling Systems", in Proceedings of the American Control Conference, July 2010, Baltimore, MD.

Mayne, D., J. Rawlings, C. Rao, and P. Scokaert. 2000. "Constrained model predictive control: stability and optimality," Automatica, Vol. 36, No. 6, pp. 789–814.

Morari, M. and J. Lee. 1999. "Model predictive control: past, present and future," Computers and Chemical Engineering, Vol. 23, pp. 667–682.

Piette, M.A.,S. Kinney, and P. Haves. Analysis of an Information Monitoring and Diagnostic System to Improve Building Operations, Energy and Buildings 33 (8) (2001), 783-791.

Radhakrishann, R., D. Nikovski, K. Peker, and A. Divakaran. Locally Weighted Regression for Fault Detection and Diagnosis of HVAC Equipment", IEEE Intl. Conf. on Industrial Electronics, 2006.

Roth, K. W., Westphalen, D., Feng, M. Y., Llana, P., and Quartararo, L. (2005). "Energy impact of commercial building controls and performance diagnostics: market characterization, energy impact of building faults and

energy savings potential". Report prepared for U.S. Department of Energy. TIAX LCC, Cambridge, MA. http://www.epa.gov/cleanenergy/energy-resources/refs.html

Sarkar, S., A. Srivastav, and M. Shashanka, "Maximally Bijective Discretization for Data-driven Modeling of Complex Systems", Proceedings of American Control Conference, (Washington, D.C.), 2013

Shengwei Wang and Youming Chen. Fault Tolerant Control for outdoor ventilation air flow rate in buildings based on neural network. Building & Environment 37 (2002) 691-704

Siroky J, Oldewurtel F, Cigler J, Privara S. 2011, "Experimental analysis of model predictive control for an energy efficient building heating system". Appl Energy. Vol. 88, pp. 3079–3087.

Soares R. d. P. and A. Secchi, European Symposium on Computer Aided Process Engineering-13, 36th European Symposium of the Working Party on Computer Aided Process Engineering, ser. Computer Aided Chemical Engineering. Elsevier, 2003, vol. 14. [Online]. Available: http://www.sciencedirect.com/science/article/pii/S1570794603802390

Wächter and L. T. Biegler, "On the Implementation of a Primal-Dual Interior Point Filter Line Search Algorithm for Large-Scale Nonlinear Programming", Mathematical Programming 106(1), pp. 25-57, 2006.

Xiong-Fu Liu and Arthur Dexter. Fault Tolerant Supervisory Control of VAV air-conditioning systems. Energy & Buildings 33 (2001) 379-389

Youmin Zhang and Jin Jiang. Bibliographical review on reconfigurable fault-tolerant control Annual Reviews in Control 32 (2008) 229–252

## ACKNOWLEDGEMENT